

Metallicity of solar-type stars with debris discs and planets ★,★

J. Maldonado¹, C. Eiroa¹, E. Villaver¹, B. Montesinos², and A. Mora³

¹ Universidad Autónoma de Madrid, Dpto. Física Teórica, Módulo 15, Facultad de Ciencias, Campus de Cantoblanco, E-28049 Madrid, Spain,

² Centro de Astrobiología (INTA-CSIC), LAEFF Campus, European Space Astronomy Center (ESAC), P.O. Box 78, E-28691 Villanueva de la Cañada, Madrid, Spain

³ ESA-ESAC Gaia SOC, P.O. Box 78, E-28691 Villanueva de la Cañada, Madrid, Spain

Received 10 January 2012; accepted 06 February 2012

ABSTRACT

Context. Around 16% of the solar-like stars in our neighbourhood show IR-excesses due to dusty debris discs and a fraction of them are known to host planets. Determining whether these stars follow any special trend in their properties is important to understand debris disc and planet formation.

Aims. We aim to determine in a homogeneous way the metallicity of a sample of stars with known debris discs and planets. We attempt to identify trends related to debris discs and planets around solar-type stars.

Methods. Our analysis includes the calculation of the fundamental stellar parameters T_{eff} , $\log g$, microturbulent velocity, and metallicity by applying the iron ionisation equilibrium conditions to several isolated Fe I and Fe II lines. High-resolution échelle spectra ($R \sim 57000$) from 2-3 meter class telescopes are used. Our derived metallicities are compared with other results in the literature, which finally allows us to extend the stellar samples in a consistent way.

Results. The metallicity distributions of the different stellar samples suggest that there is a transition toward higher metallicities from stars with neither debris discs nor planets to stars hosting giant planets. Stars with debris discs and stars with neither debris nor planets follow a similar metallicity distribution, although the distribution of the first ones might be shifted towards higher metallicities. Stars with debris discs and planets have the same metallicity behaviour as stars hosting planets, irrespective of whether the planets are low-mass or gas giants. In the case of debris discs and giant planets, the planets are usually cool, - semimajor axis larger than 0.1 AU (20 out of 22 planets), even $\approx 65\%$ have semimajor axis larger than 0.5 AU. The data also suggest that stars with debris discs and cool giant planets tend to have a low dust luminosity, and are among the less luminous debris discs known. We also find evidence of an anticorrelation between the luminosity of the dust and the planet eccentricity.

Conclusions. Our data show that the presence of planets, not the debris disc, correlates with the stellar metallicity. The results confirm that core-accretion models represent suitable scenarios for debris disc and planet formation. These conclusions are based on a number of stars with discs and planets considerably larger than in previous works, in particular stars hosting low-mass planets and debris discs. Dynamical instabilities produced by eccentric giant planets could explain the suggested dust luminosity trends observed for stars with debris discs and planets.

Key words. techniques: spectroscopic - stars: abundances - stars: circumstellar matter - stars: late-type - stars: planetary systems

1. Introduction

Understanding the origin and evolution of planetary systems is one of the major goals of modern astrophysics. The unexpected discovery by the *IRAS* satellite of infrared excesses around main-sequence stars (Aumann et al. 1984) was attributed to the presence

Send offprint requests to: J. Maldonado,
e-mail: jesus.maldonado@uam.es

* Based on observations collected at the Centro Astronómico Hispano Alemán (CAHA) at Calar Alto, operated jointly by the Max-Planck Institut für Astronomie and the Instituto de Astrofísica de Andalucía (CSIC); observations made with the Italian Telescopio Nazionale Galileo (TNG) operated on the island of La Palma by the Fundación Galileo Galilei of the INAF (Istituto Nazionale di Astrofisica); observations made with the Nordic Optical Telescope, operated on the island of La Palma jointly by Denmark, Finland, Iceland, Norway, and Sweden, in the Spanish Observatorio del Roque de los Muchachos of the Instituto de Astrofísica de Canarias; and data obtained from the ESO Science Archive Facility.

** Tables 1 and 4 are only available in the electronic version of the paper or at the CDS via anonymous ftp to cdsarc.u-strasbg.fr (130.79.128.5) or via <http://cdsweb.u-strasbg.fr/cgi-bin/qcat?J/A+A/>

ence of faint dusty discs, produced by collisional events within a significant population of invisible left-over planetesimals. The discovery of these so-called *debris discs* demonstrated that planetesimals are more common than had been previously thought, revealing that the initial steps of planetary formation are ubiquitous (e.g. Backman & Paresce 1993). This realisation has been complemented in the past 15 years with the detection of more than 700 exoplanets orbiting stars other than the Sun¹.

More recent studies have found that more than 50% of solar-type stars harbor at least one planet of any mass with a period of up to 100 days, and about 14% of this type of stars have planetary companions more massive than $50 M_{\oplus}$ with periods shorter than 10 years (Mayor et al. 2011). It is well-established that the percentage of stars hosting gas-giant planets increases with the metal content, up to 25% for stars with metallicities higher than +0.30 dex (e.g. Santos et al. 2004; Fischer & Valenti 2005). On the other hand, stars that host less massive planets, Neptune-like or super Earth-like planets ($M_p < 30 M_{\oplus}$), do not tend to be metal-rich (Ghezzi et al. 2010b; Mayor et al. 2011;

¹ <http://exoplanet.eu/>

Sousa et al. 2011, and references therein). In terms of the metallicity of evolved stars (late-type subgiants and red giants) hosting planets, previous results have been based on the analysis of small and inhomogeneous samples that even produce contradictory results, while these stars are metal-poor in the cases of Pasquini et al. (2007) and Ghezzi et al. (2010a), they show metal enrichment according to Hekker & Meléndez (2007).

Debris discs are, strictly speaking, signatures of planetesimal systems. About 16% of the main-sequence solar-like (spectral types F5-K5) stars are known to show an excess at $70\text{ }\mu\text{m}$ (e.g. Trilling et al. 2008). If planetesimals were the building blocks of planets and, at the same time, the raw material from which debris discs form, their host stars might be expected to have similar properties. However, the incidence of debris discs is no higher around planet-host stars than around stars without detected planets (Kóspál et al. 2009), and several works do not find any correlation between the presence of a debris disc and the metallicity, or any other characteristic, of the stars with planets (e.g. Beichman et al. 2005; Chavero et al. 2006; Greaves et al. 2006; Moro-Martín et al. 2007; Bryden et al. 2009; Kóspál et al. 2009).

In this paper, we revisit the analysis of the properties of solar-type stars hosting planets and/or debris discs. One of the motivations is the increase with respect to previous works of $\sim 50\%$, in the number of stars with known debris discs and planets, in particular those associated with low-mass planets ($M_p \lesssim 30M_{\oplus}$). We distinguish three different categories: stars with known debris discs but no planets (SWDs hereafter), stars with known debris discs and planets (SWDPs), and stars with known planets but no discs (SWPs). In addition, we consider a comparison sample of stars with no detected planets and no detected debris discs (SWODs). We use our own high-resolution échelle spectra to homogeneously determine some of the stellar properties, particularly metallicity, and in a second step we compare our spectroscopic results with published results. This allows us to increase coherently the stellar samples analysed in this work.

2. Observations

2.1. The stellar sample

A list of stars with known debris discs, SWDs, was compiled by carefully checking the works of Habing et al. (2001), Spangler et al. (2001), Chen et al. (2005), Beichman et al. (2006), Bryden et al. (2006), Moór et al. (2006), Smith et al. (2006), Moro-Martín et al. (2007), Rhee et al. (2007), Trilling et al. (2007), Trilling et al. (2008), Bryden et al. (2009), Kóspál et al. (2009), Plavchan et al. (2009), Tanner et al. (2009), Koerner et al. (2010), Dodson-Robinson et al. (2011), and Moór et al. (2011). These debris discs were discovered by the *IRAS*, *ISO*, and *Spitzer* telescopes. We compiled a total list of 305 stars, from which we retained for study only the solar-type stars (Hipparcos spectral type between F5 and K2-K3), leading to a total of 136 stars. Most of the debris discs around these stars were detected at *Spitzer*-MIPS $70\text{ }\mu\text{m}$, with fractional dust luminosities of the order of 10^{-5} and higher (Trilling et al. 2008).

To build the *comparison* sample of stars without discs (SWODs), we selected from the aforementioned works stars in which IR-excesses were not found at 24 and $70\text{ }\mu\text{m}$ by *Spitzer*. As before, only solar-type stars were considered, leading to 150 stars. Since *Spitzer* is limited up to fractional luminosities of $L_{\text{dust}}/L_{\star} \gtrsim 10^{-5}$, we cannot rule out the possibility that some of these stars have fainter discs.

Table 1. The SWD and SWOD samples. Only the first eight lines of the SWD sample and the references are presented here; the full version of the table is available as online material.

HIP	HD	SpType	V	distance (pc)	log(Age) (yr)	[Fe/H] [†] (dex)	Ref
Stars with known debris discs.							
171	224930	G3V	5.80	12.17	9.60	-0.72 (a)	13
490	105	G0V	7.51	39.39	8.34	-0.03 (b)	2
544	166	K0V	6.07	13.67	9.16	0.15 (a)	5
682	377	G2V	7.59	39.08	8.34	0.12 (b)	6
1481	1466	F8/G0	7.46	41.55	8.34	-0.22 (c)	7
1598	1562	G0	6.97	24.80	9.79	-0.32 (a)	13
1599	1581	F9V	4.23	8.59	9.58	-0.29 (a)	9
2843	3296	F5	6.72	45.05		0.02 (c)	9

[†] (a) This work; (b) Valenti & Fischer (2005); (c) Nordström et al. (2004)

(b) and (c) values are set into our metallicity scale as described in Section 3.2.

(1) Habing et al. (2001); (2) Spangler et al. (2001); (3) Chen et al. (2005);

(4) Beichman et al. (2006); (5) Bryden et al. (2006); (6) Moór et al. (2006);

(7) Smith et al. (2006); (8) Rhee et al. (2007); (9) Trilling et al. (2008);

(10) Kóspál et al. (2009); (11) Plavchan et al. (2009); (12) Tanner et al. (2009);

(13) Koerner et al. (2010); (14) Moór et al. (2011),

Table 2. Comparison between the properties of the SWDs and the SWODs samples.

	SWDs			SWODs		
	Range	Mean	Median	Range	Mean	Median
Distance (pc)	3.6/134	32.0	24.6	5.8/53	24.1	20.6
log[Age (yr)]	7.2/9.9	9.0	9.0	7.6/9.9	9.2	9.6
SpType (%)	45.8 (F); 34.6 (G); 19.6 (K)			42.8 (F); 44.8 (G); 12.4 (K)		

To avoid the effects of planets, planet-hosting stars in both the SWD and SWOD samples were removed, after checking the Extrasolar Planets Encyclopedia². The final number of stars in the SWDs sample is 107: 49 F-type stars, 37 G-type stars, and 21 K-type stars. The SWODs sample contains 145 stars: 62 F-type stars, 65 G-type stars, and 18 K-type stars. Table 1 lists the stars in the SWD and SWOD samples, their properties, and references to debris disc detection.

2.2. Possible biases

Metallicity reflects the enrichment history of the ISM (see e.g. Timmes et al. 1995). It is, therefore, important to determine whether the SWD and SWOD samples have randomly selected stellar hosts in terms of age and distance, which are the parameters most likely to affect the metal content of a star. In this respect, we compared the distances and stellar ages of both samples; the results are given in Table 2. Distances are from the updated Hipparcos parallaxes (van Leeuwen 2007) and stellar ages were computed from the log R'_{HK} values given by Maldonado et al. (2010) or from the literature if no value was available in that work. The relationship provided by Mamajek & Hillenbrand (2008, Eq. 3) was used to compute the ages. This relationship has an accuracy of 15-20% for young stars, i.e. younger than 0.5 Gyr, and at older age, uncertainties can grow by up to 60%. The age distributions are shown in Figure 1.

We found a difference between the two samples in terms of the age, with the SWDs containing 15% more stars younger than 500 Myr. Type II and Type Ia supernova (SNe) are the two sources of Fe production, each operating on different timescales

² <http://exoplanet.eu/>

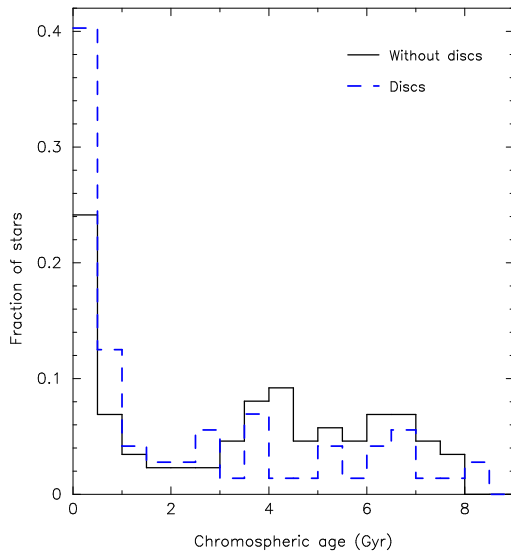


Fig. 1. Age distribution for stars in the SWOD (continuous-black line) and the SWD (dotted-blue line) samples.

and accounting for very different amounts of the total Fe injected into the ISM. While Type Ia SNe are the major producers of Fe in galaxies (see e.g. Matteucci & Greggio 1986), their injection timescales are, according to the most recent estimates, longer than 1 Gyr (Matteucci et al. 2009). In the solar neighbourhood, this 1 Gyr timescale, although uncertain, is the time at which the Fe production from SNe Ia starts to become important (Matteucci & Recchi 2001). On the other hand, Type II SNe are expected to account for only 30% of the total yield of Fe (Matteucci & Greggio 1986) but are expected to do so on a shorter timescale (3-5 Myr). A high rate of local SN type II explosions has been estimated to explain the local bubble (Maíz-Apellániz 2001), namely 20 SN type II explosions within 150 pc of the Sun in the past 11 Myr (Benítez et al. 2002). The youngest stars in the SWD and SWOD samples have ages of 15 Myr and 35 Myr, respectively, with a larger number of young SWDs in the first 500 Myr bin. The paucity of SNe type II in the Galaxy (typical rate of ≈ 1 SNe Myr $^{-1}$) and all the stars being at relatively close distances from the Sun (less than 130 pc) make it very unlikely that the two samples have experienced different enrichment histories. We have, however, explored this possibility in Figure 2, where we plot the metallicity versus age (Section 3) for the two samples. As we can see, the SWDs and SWODs have similar behaviours. Young stars in the SWDs sample do not seem to have higher metallicities, so we can rule out a possible chemical evolution in the SWD sample.

We have also checked whether there is a difference between the SWD and SWOD samples in terms of distance that might affect their metallicity distributions. After all, the SWD sample contains stars out to a larger volume than that of the SWODs and could possibly include stars with a different chemical evolution. Garnett & Kobulnicky (2000) studied the scatter in the age-metallicity relation for F and G dwarf stars in the solar neighbourhood up to 80 pc, and found that their stars at distances 30-80 pc from the Sun are more metal-poor than those within 30 pc. Garnett & Kobulnicky (2000) attributed this difference to the possible consequence of a selection bias in the analysed sample.

We certainly cover the same volume of stars in our homogeneous SWD and SWOD subsamples (see Section 3.1), since they are located within 25 pc of the Sun (Maldonado et al. 2010). We do not find any chemical distinction between these two subsam-

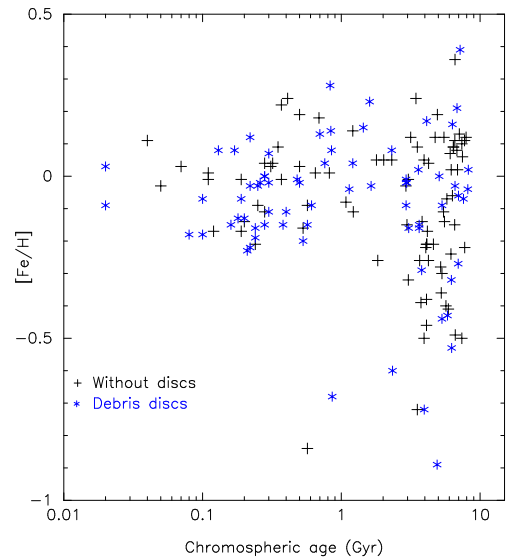


Fig. 2. [Fe/H] versus age for the stars in the SWOD (black crosses) and in the SWD (blue asterisks) samples.

ples. If in the full sample (see Section 3.3) we had a selection bias due to the larger distance of the SWODs, we would expect its metallicity distribution to show a larger dispersion owing to a possible contamination by stars not born in the solar neighbourhood. We have the opposite case, where the full samples of both SWODs and SWDs have a smaller dispersion than the volume-limited homogeneous SWDs and SWODs subsamples (see Figure 3).

In short, we believe that we have a randomly selected sample of stars in terms of their chemical history, although the SWD and SWOD samples show some differences in age and distance.

2.3. Spectroscopic observations

The high-resolution spectra used in this work are the same as in Maldonado et al. (2010), where a complete description of the observing runs and the reduction procedure can be found. In brief, the data were taken with the following spectrographs and telescopes: i) FOCES (Pfeiffer et al. 1998) at the 2.2 meter telescope of the Calar Alto observatory (Almería, Spain); ii) SARG (Gratton et al. 2001) at the TNG, La Palma (Canary Islands, Spain); and iii) FIES (Frandsen & Lindberg 1999) at the NOT, La Palma. We also used additional spectra from the public library “S⁴N” (Allende Prieto et al. 2004), which contains spectra taken with the 2dcoudé spectrograph at McDonald Observatory and the FEROS instrument at the ESO 1.52 m telescope in La Silla, and from the ESO/ST-ECF Science Archive Facility³ (specifically FEROS spectra). Table 3 lists the spectral range and resolving power of each of the spectrographs. The number of stars covered by these spectra are 35 (33%) and 58 (40%) for the SWD and SWOD samples, respectively. Thus, we consider additional data from the literature to analyse the whole set of stars in both samples (see Section 3.3).

2.4. Analysis

The stellar parameters T_{eff} , $\log g$, microturbulent velocity (ξ_t), and [Fe/H], are determined using the code TGV developed by Takeda et al. (2002), which is based on iron-ionisation equilib-

³ <http://archive.eso.org/cms/>

Table 3. Properties of the different spectrographs used in this work.

Spectrograph	Spectral range (Å)	Resolving power
FOCES	3470-10700	57000
SARG	5500-10100	57000
FIES	3640-7360	67000
FEROS	3500-9200	42000
Mc Donald	3400-10900	60000

Table 4. Fe I and Fe II lines used to compute abundances. Wavelengths are given in Angstroms (Å).

	Fe I		Fe II
4389.25	6173.34	6699.14	4576.34
4445.48	6180.21	6739.52	4620.52
5225.53	6200.32	6750.16	4656.98
5247.06	6219.29	6752.71	5234.63
5250.22	6232.65	6793.27	5264.79
5326.15	6240.65	6804.00	5414.08
5412.79	6265.14	6804.28	5525.13
5491.84	6271.28	6837.01	6432.68
5600.23	6280.62	6854.83	6516.08
5661.35	6297.80	6945.21	7222.40
5696.09	6311.51	6971.94	7224.46
5701.55	6322.69	6978.86	7515.84
5705.47	6353.84	7112.17	7711.73
5778.46	6481.88	7401.69	
5784.66	6498.95	7723.21	
5855.08	6518.37	7912.87	
5909.98	6574.23	8075.16	
5956.70	6581.21	8204.11	
6082.72	6593.88	8293.52	
6120.26	6609.12	8365.64	
6137.00	6625.03		
6151.62	6667.72		

rium conditions, a methodology that is widely applied to solar-like stars (spectral types F5/K2-K3). Iron abundances are computed for a well-defined set of Fe I and Fe II lines. Basically, the stellar parameters are adjusted until: i) no dependence is found between the abundances derived from Fe I lines and the lower excitation potential of the lines; ii) no dependence is found between the abundances derived from the Fe I lines and their equivalent widths; and iii) the derived mean Fe I and Fe II abundances are the same. We list the lines used in Table 4. We are aware that ideally all our targets should have been observed with the same spectrograph using the same configuration. Nevertheless, all the spectra used here have a similar resolution, and cover enough Fe lines to provide a high-quality metallicity determination. Only for the SARG spectra is the number of Fe II lines slightly lower (6 out of 13, begining in the 6432.68 Å line).

Equivalent widths are obtained by fitting the lines with a Gaussian profile using the IRAF⁴ task *splot*. Stars with significant rotational velocities, $v \sin i$, have lines affected by blending, complicating the application of this method. Stars with $v \sin i \gtrsim 15\text{-}20 \text{ km s}^{-1}$ typically do not have enough isolated lines to obtain accurate parameters. This has a small impact on our estimates since we consider stars with spectral types

⁴ IRAF is distributed by the National Optical Astronomy Observatory, which is operated by the Association of Universities for Research in Astronomy, Inc., under contract with the National Science Foundation.

F5 or later, with typical $v \sin i$ values in the range 3-9 km s^{-1} (Martínez-Arnáiz et al. 2010). The estimated stellar parameters and iron abundances are given in Table 5.

3. Results

3.1. Homogeneous analysis

In a first step, we consider the 35 SWDs and 58 SWODs whose metallicities were estimated directly in this work. The stars in these *homogeneous samples* are listed in Table 5, and are marked in Column 7 of Table 1 as well. Figure 3 (left panel) shows the normalized distribution of these stars. Both distributions are very similar. The metallicity distribution of the SWOD sample spreads over a large range containing both metal-poor and metal-rich stars, from -1.12 to 0.36 dex. The mean metallicity of the distribution is -0.09 dex with an RMS dispersion of 0.27 dex. The distribution of the SWDs spans a slightly narrower range, from -0.89 to 0.35 dex, with a mean value of -0.10 dex and a dispersion of 0.28 dex. Since the mean of a distribution is strongly affected by the presence of outliers, we consider the median as a more representative value. The median values for the SWOD and SWD distributions are -0.01 and -0.02, respectively. To assess whether both distributions are equal from a statistical point of view, a two-sample Kolmogorov-Smirnov (K-S) test was performed (details about how the K-S test is applied in this paper are given in Appendix A). The maximum difference between the SWD and SWOD cumulative distribution functions is only ~ 0.11 , while the likelihood that both samples have the same parent distribution is around 94%.

3.2. Comparison with previous works

The spectroscopic observations performed by Maldonado et al. (2010) were limited to 25 pc in distance and, therefore, do not cover all SWDs and SWODs in Table 1. Thus, we use the data of Nordström et al. (2004, NO04), Valenti & Fischer (2005, VF05) and Takeda et al. (2005, TA05) to analyse the full samples. To ensure that we did not introduce any bias resulting from estimates based on different analysis techniques, a comparison between our metallicities and the ones reported in these papers is shown in Figure 4. Our sample contains 72 stars in common with NO04. Our metallicities are slightly higher, by a factor ~ 0.07 dex (in median), than those given by NO04; the differences are largest for stars with positive metallicities. The agreement with VF05 is very good, with no apparent bias for the 64 stars in common; the mean difference is only -0.01 dex with a standard deviation of 0.09 dex. The VF05 metallicities are also higher than the NO04 values by a factor ~ 0.08 dex. The agreement with TA05 is excellent, better than ± 0.10 dex for most of the 49 common stars. The latter result is expected because the same method and lines were used to estimate the metallicity; it can thus be considered a consistency double check.

3.3. Full sample

To set the VF05 and NO04 metallicities on our own metallicity scale, we used the stars in common to obtain a linear transformation (Figure 4). Where possible, VF05 values were selected because they have been obtained from high-resolution spectra similar to those used in this work. The metallicities in NO04 are based on Strömgren *uvbyβ* photometry. The adopted final metallicity values for each star of the SWD and SWOD samples are given in Table 1.

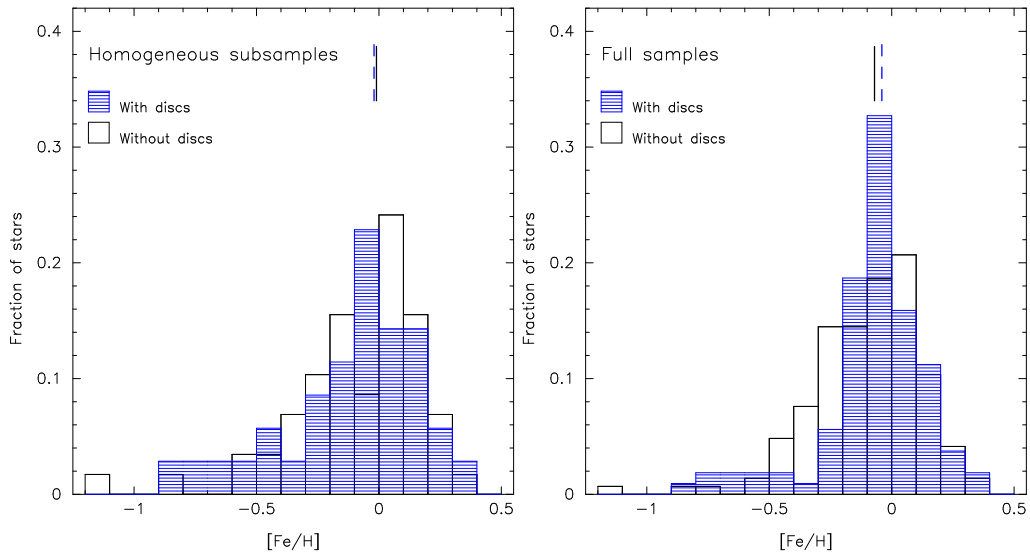


Fig. 3. Normalized metallicity distribution of the stars without debris discs (SWODs, empty histogram), and the stars with debris discs (SWDs, blue histogram shaded at 0 degrees). Median values of the distributions are shown with vertical lines. Left panel: distributions of the stars in the homogeneous sample, i.e., metallicities computed from our own spectra. Right panel: distributions of the full stellar sample (see text).

Table 5. Estimated physical parameters with uncertainties for the stars measured in this work. Columns 8 an 10 give the mean iron abundance derived from Fe I and Fe II lines, respectively, while columns 9 and 11 give the corresponding number of lines. The rest of the columns are self-explanatory. Only the first eight lines are shown here; the full version of the table is available online.

HIP	HD	SpType	T _{eff} (K)	log g (cm s ⁻²)	ξ_t (km s ⁻¹)	[Fe/H] dex	$\langle A(\text{Fe I}) \rangle$	n _I	$\langle A(\text{Fe II}) \rangle$	n _{II}	Spec. [†]
(1)	(2)	(3)	(4)	(5)	(6)	(7)	(8)	(9)	(10)	(11)	(12)
Stars with known debris discs.											
171	224930	G3V	5491 ± 31	4.75 ± 0.12	0.92 ± 0.40	-0.72 ± 0.08	6.78 ± 0.11	52	6.78 ± 0.12	12	4
544	166	K0V	5575 ± 51	4.68 ± 0.14	1.05 ± 0.25	0.15 ± 0.05	7.65 ± 0.06	57	7.65 ± 0.06	13	4
1598	1562	G0	5603 ± 36	4.30 ± 0.12	0.67 ± 0.27	-0.32 ± 0.06	7.18 ± 0.07	58	7.18 ± 0.09	12	1
1599	1581	F9V	5809 ± 39	4.24 ± 0.12	1.30 ± 0.30	-0.29 ± 0.06	7.21 ± 0.08	59	7.22 ± 0.10	13	5
5336	6582	G5V	5291 ± 32	4.57 ± 0.11	0.82 ± 0.42	-0.89 ± 0.08	6.61 ± 0.11	55	6.62 ± 0.12	12	4
5862	7570	F8V	6111 ± 35	4.42 ± 0.10	1.35 ± 0.17	0.17 ± 0.03	7.67 ± 0.04	50	7.67 ± 0.04	13	6
5944	7590	G0	5951 ± 39	4.65 ± 0.11	1.04 ± 0.38	-0.02 ± 0.05	7.48 ± 0.06	48	7.48 ± 0.08	11	1
7576	10008	G5	5293 ± 68	4.90 ± 0.19	0.39 ± 0.45	0.08 ± 0.06	7.58 ± 0.07	53	7.58 ± 0.10	9	1

[†]Spectrograph: (1) CAHA/FOCES; (2) TNG/SARG; (3) NOT/FIES; (4) S⁴N-MCD; (5) S⁴N-FEROS; (6) ESO/FEROS

Some statistical diagnostics for the SWD and SWOD full samples are summarised in Table 6. Both samples have similar distributions. The *full* SWD distribution has a median of -0.04 dex, very close to the value obtained in the *homogeneous* analysis (-0.02 dex). In the case of the SWOD sample, the *full* sample has a median of -0.07 dex that, when compared with the value of -0.01 dex for the *homogeneous* subsample, means a difference of 0.06 dex. We note that 0.06 dex is of the order of the individual uncertainties in metallicity. The SWD and SWOD distributions have a smaller dispersion when we consider the whole sample (Figure 3, right panel). Using a K-S analysis, we tested the possibility of both distributions to differing within a 98% confidence level; our results cannot exclude that both samples come from the same parent distribution at this confidence level. Nevertheless, the likelihood that both samples are drawn from the same parent distribution diminishes significantly with respect to the homogeneous sample case (9%, see Appendix A). An interesting aspect is that there seems to be a “deficit” of stars with discs in the metallicity range $-0.50 < [\text{Fe/H}] < -0.20$. This

Table 6. [Fe/H] statistics of the stellar samples

Sample	Mean	Median	Deviation	Min	Max	N
SWODs	-0.09	-0.07	0.22	-1.12	0.36	145
SWDs	-0.08	-0.04	0.26	-1.49	0.39	107
SWDPs	0.08	0.05	0.17	-0.34	0.36	29
SWPs	0.10	0.15	0.22	-0.70	0.43	120

deficit is not explicit in the homogeneous case (Figure 3, see also Section 4 and Figure 7).

3.4. Stars with known debris discs and planets

At the time of writing⁵, there are, to our knowledge, 29 solar-type stars known to host both a debris disc and at least one planet (SWDPs). This figure represents an increase of $\sim 50\%$ with re-

⁵ December 26, 2011

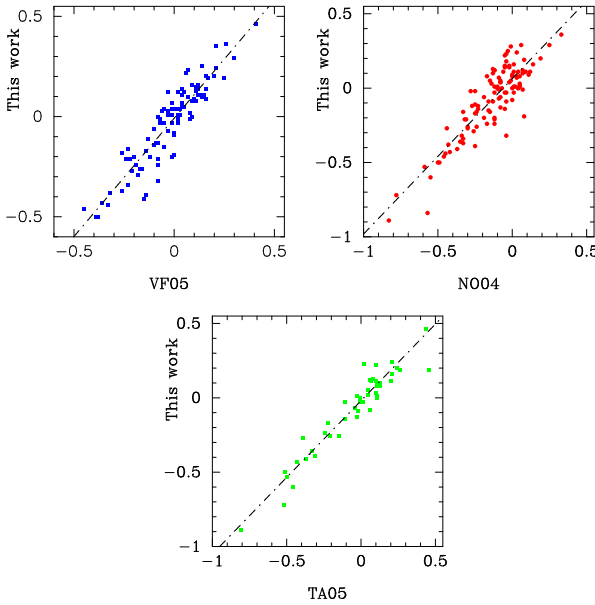


Fig. 4. Comparison between the metallicities from the literature and those obtained in this work. Top left panel: VF05; top right panel: NO04; bottom panel: TA05. Dashed lines represent the best linear fit ($y = m^*x + b$) between our metallicities and those given in the corresponding works. The coefficients are: $m=1.18 \pm 0.05$, $b = -0.008 \pm 0.008$ for VF05; $m=1.04 \pm 0.05$, $b = 0.064 \pm 0.013$ for N04; and $m=0.99 \pm 0.05$, $b = -0.017 \pm 0.011$ for TA05.

spect to the most recent works (Bryden et al. 2009; Kóspál et al. 2009)⁶. These stars are listed in Table 7.

Among the 29 SWDPs, 11 stars host known multiplanet systems, which represents an incidence rate of 38%. Wright et al. (2009) found a rate of 14% confirmed multiple planetary systems, and it could be 28% or higher when they include cases with a significant evidence of being multiple⁷. Mayor et al. (2011) found a rate exceeding 70% among their 24 systems with planets less massive than $30 M_{\oplus}$. In our SWDP sample, there are five stars with low-mass planets in multiple systems, but this might be a lower limit, as pointed out by Mayor et al. (2011). This suggests that the multiplanet system rate in SWDPs approaches that of the low-mass planet case.

There are 7 of 29 SWDPs that host at least one low-mass planet, $M \lesssim 30 M_{\oplus}$. These stars are HD 1461, HD 20794, HD 38858, HD 45184, HD 69830, 61 Vir (HD 115617), and HD 215152; in all cases, but in HD 1461, their metallicity is $[Fe/H] \leq 0.0$, consistent with the metallicity trend for stars with low-mass planets (e.g. Mayor et al. 2011; Sousa et al. 2011).

Wright et al. (2009, Figure 9) and Currie (2009, Figure 1) showed that there is an enhanced frequency of close-in gas giant planets with semimajor axes $\lesssim 0.07$ AU (hot Jupiters). Among the 22 SWDPs that are currently known to host only gas-giant planets, HD 46375 is the only star harbouring such a close-in planet, semimajor axis of 0.041 AU, while HD 130322 has a hot Jupiter at 0.088 AU; five more stars have giant planets with

⁶ For the 22 stars with debris discs and planets given by Kóspál et al. (2009), HD 33636 has a substellar companion that has been retracted as a planet (Bean et al. 2007), GJ 581 is a M star, and HD 137759 is a giant star. In addition, Bryden et al. (2009) listed HD 150706 as hosting a planet and a debris disc, but the planet is not confirmed (<http://exoplanet.eu>).

⁷ See also for comparison <http://exoplanet.eu>

Table 7. Stars with known debris discs and planets.

HIP	HD	SpType	[Fe/H] [†] (dex)	Ref [‡]	Planet [*]
522	142	F7V	0.09 (b)	9:	gc
1499	1461	G0V	0.18 (b)	11	mlh
7978	10647	F8V	-0.09 (a)	3	gc
14954	19994	F8V	0.19 (a)	8	gc
15510	20794	G8V	-0.34 (a)	10	mhc
16537	22049	K2V	-0.08 (a)	1	gc
27253	38529	G4V	0.31 (b)	6	mhc
27435	38858	G4V	-0.27 (a)	4	lc
28767	40979	F8	0.13 (b)	10:	gc
30503	45184	G2V	0.03 (b)	11	lh
31246	46375	K1IV	0.23 (b)	10:	gh
32970	50499	G1V	0.29 (b)	10:	gc
33212	50554	F8	-0.09 (b)	8	gc
33719 [#]	52265	G0V	0.18 (b)	8	gc
40693	69830	K0V	0.00 (a)	2	mlh
42282	73526	G6V	0.22 (b)	10:	mhc
47007	82943	G0	0.23 (b)	8	mhc
58451	104067	K2V	0.04 (b)	11	gc
61028	108874	G5	0.17 (b)	12	mhc
64924	115617	G5V	0.00 (a)	8	mlh
65721	117176	G5V	-0.03 (a)	8	gc
71395	128311	K0	0.04 (a)	8	mhc
72339	130322	K0V	-0.07 (b)	12	gh
94075	178911B	G5	0.29 (b)	10:	gc
97546	187085	G0V	0.05 (b)	10:	gc
99711	192263	K2	-0.01 (a)	5	gc
104903	202206	G6V	0.36 (b)	10	mhc
112190	215152	K0	-0.10 (c)	11	mlh
113044	216435	G3IV	0.24 (b)	10	gc

[†] (a) This work; (b) Valenti & Fischer (2005)

[‡] values are set into our metallicity scale as described in Section 3.2.

^{*} (c) Metallicity for this star is from Sousa et al. (2008) since no value were found in VF05 or NO04.

[#] (1) Habing et al. (2001); (2) Bryden et al. (2006);

(3) Moór et al. (2006); (4) Beichman et al. (2006);

(5) Smith et al. (2006); (6) Moro-Martín et al. (2007);

(7) Rhee et al. (2007); (8) Trilling et al. (2008);

(9) Bryden et al. (2009); (10) Kóspál et al. (2009);

(11) Koerner et al. (2010); (12) Dodson-Robinson et al. (2011)

The symbol “:” means that non-excess is attributed to the corresponding star in (9) or (10).

* m = multiplanet system; l = low-mass planet;

g = gas giant planet; c = cool planet;

h = hot planet (semimajor axis ≤ 0.1 AU, see text);

[#] Spectral type from Montes et al. (2001)

semimajor axes smaller than 0.5 AU (HD 38529, HD 104067, HD 117176, HD 178911B, and HD 192263). On the other hand, the semimajor axes of the low-mass planets are $\lesssim 0.07$ AU in all cases, but in HD 20794 and HD 38858.

The statistical properties of the SWDP metallicity distribution are shown in Table 6, while Figure 5 (left) compares the corresponding SWDP histogram with the SWDs. The figure clearly shows the distinct metallicity distributions of both the SWDPs and the SWDs; a K-S test confirms that both distributions differ within a confidence level of 98% (the likelihood of being the same distribution is 0.7%).

Summarizing, although there may be some bias related to the planet detection methods as well as the sensitivity in detecting debris discs, our results suggest that SWDPs i) have higher

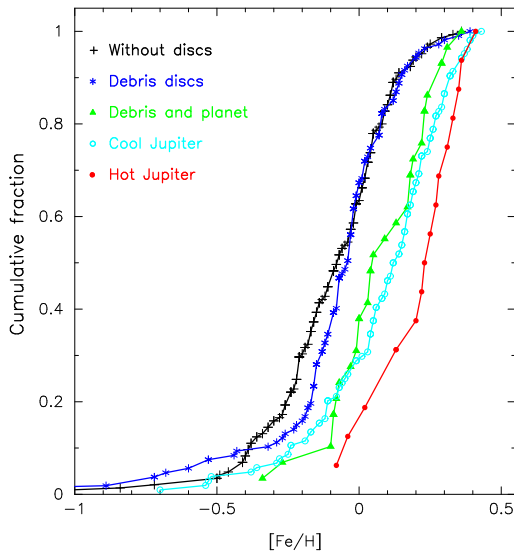


Fig. 7. Histogram of cumulative frequencies for the different samples studied in this work.

metallicities than both SWDs and SWODs (see Figures 5 and 7), ii) they tend to have a higher incidence of multiplanet systems, most likely at a rate close to the one of stars with low-mass planets, iii) many of them host low-mass planets, and iv) in the cases with only gas-giant planets, these planets tend to be cool Jupiters (only two out of 22 stars harbour one hot Jupiter).

3.5. Comparison with stars with giant planets

Figure 5 (right) shows the metallicity distributions of both SWDPs and SWPs. The SWPs sample contains 120 stars and corresponds to stars hosting exclusively giant planets from Santos et al. (2004), Valenti & Fischer (2005), Sousa et al. (2011), and Mayor et al. (2011), where we have removed the stars with retracted or not-confirmed exoplanets. Both histograms clearly show that the stars in the SWP and SWDP samples tend to have high metallicity. The K-S tests cannot rule out that both distributions are the same (p -value = 49%).

With the aim of completeness, Figure 6 compares the metallicity distribution of the SWPs, with those of the SWODs and SWDs samples, where the well-known trend of SWPs (gas-giant planets) to higher metallicities is clearly reproduced.

4. Discussion

The results presented in the previous section suggest that a transition toward higher metallicities occurs from SWODs to SWPs. The cumulative metallicity distributions, presented in Figure 7, allow us to get an unified overview of the metallicity trends. As pointed out before, the distribution of SWDs is similar to that of SWODs, but there seems to be a deficit of SWDs at low $[Fe/H]$, below approximately -0.1 (see also the histogram for the full samples in Figure 3 (right panel) and the median $[Fe/H]$ value in Table 6). The distribution of SWDPs can be clearly distinguished from that of SWDs and is similar to that of SWPs. Thus, planets are clearly the main drivers of the trend in stellar metallicity in SWDPs; this is true for both the low-mass and the giant planets in the SWDP sample. The metallicity distribution of SWPs was divided into hot and cool Jupiters because most of the SWDPs hosting giant planets are associated with cool planets. Figure 7 suggests that the frequency of hot giant planets is

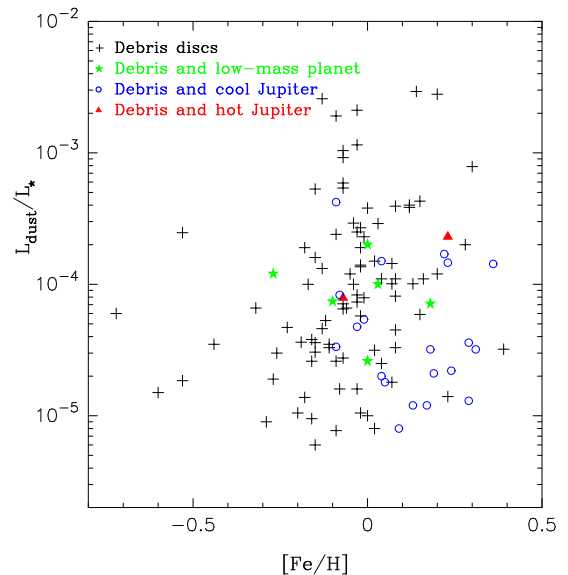


Fig. 8. Fractional dust luminosity, L_{dust}/L_* , versus $[Fe/H]$ for those stars hosting a debris discs. Stars are plotted with different symbols and colours depending on the presence/absence of low-mass or cool/hot Jupiter planets.

lower for low metallicities than the frequency of cool ones. We point out that a similar trend is obtained, when the data refer to all known solar-type stars hosting giant planets, i.e., stars with close-in giant planets tend to be more metal-rich.

These trends can be explained by core-accretion models (e.g. Pollack et al. 1996; Ida & Lin 2004; Hubickyj et al. 2005; Mordasini et al. 2009, 2012), and are consistent with the view that the mass of solids in proto-planetary discs is the main factor controlling the formation of planets and planetesimals (Greaves et al. 2007; Moro-Martín et al. 2007). Thus, the rapid build-up of a core in a metal-rich proto-planetary disc would allow giant planets to form before the dissipation of the gas, while the formation of planetesimals could proceed slowly after the gas dissipation and also in a less metal-rich environment. We note that planetesimals could form regardless of the giant planet formation, and that the timescale for Earth-like planet formation is long and can proceed in a relatively metal-poor environment.

Figure 8 shows the fractional dust luminosity, L_{dust}/L_* , of the SWDs and SWDPs versus the metallicity. The plot distinguishes between low-mass and gas giant planets. Values of L_{dust}/L_* are taken from the references in Section 2.1; we plot the mean value of L_{dust}/L_* for the stars from Trilling et al. (2008). It is found that the SWDPs as a whole span approximately two orders of magnitude in L_{dust}/L_* and are well-mixed with SWDs, while most of the stars hosting debris discs and cool giant planets tend to have low dust luminosities, $L_{dust}/L_* < 10^{-4}$; more than 50% of SWDPs of this type are indeed concentrated in the low-dust luminosity/high-metallicity corner of Figure 8. In addition, there seems to be a trend of larger eccentricities (we take as reference the innermost planet) while the luminosity of the dust decreases, albeit with a large scatter (Figure 9). Such an anticorrelation may be the result of dynamical instabilities produced by eccentric giant planets, which clear out the inner and outer regions of the planetary discs (Raymond et al. 2011). On the other hand, there is no trend with the semimajor axis of the planet (not shown), although it seems that low-mass planets tend to be predominantly hot but most of the giant planets are cool (Section 3.4). Furthermore, while the SWDs span the \sim 10 Myr - 10 Gyr range,

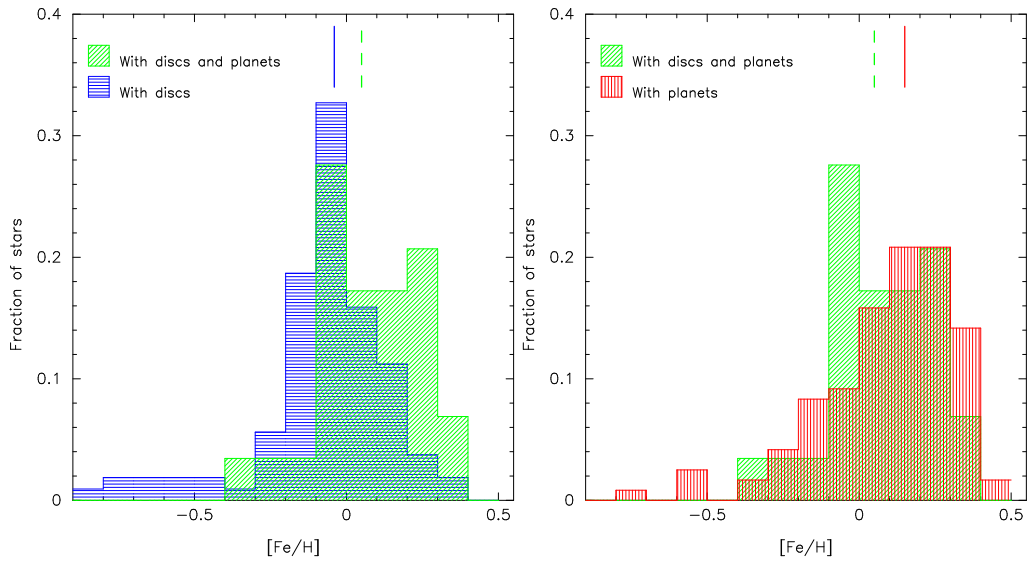


Fig. 5. Normalized metallicity distribution of the SWDP sample (light green histogram) versus stars with debris discs (left) and stars with giant planets (right). Median values of the distributions are shown with vertical lines.

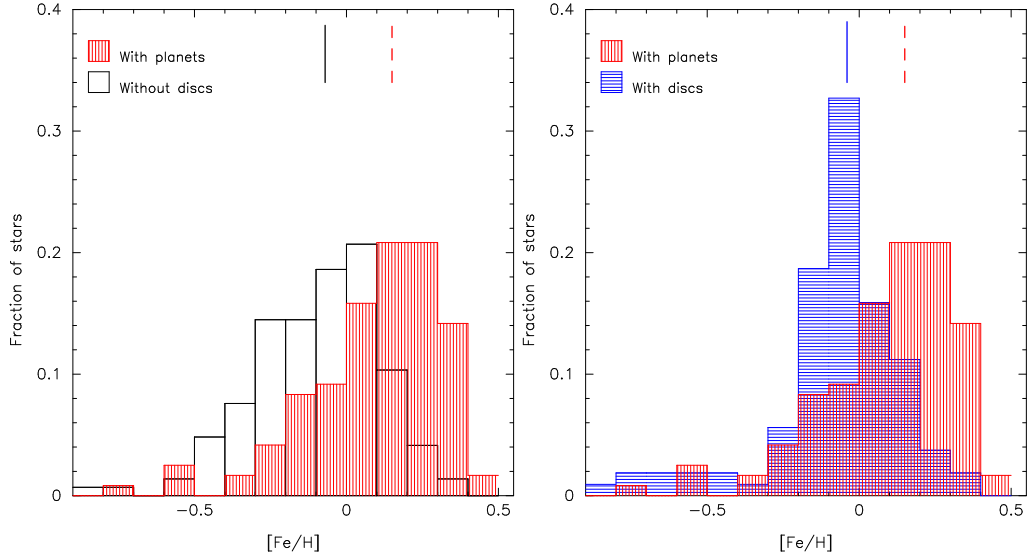


Fig. 6. Normalized metallicity distributions of planet host-stars (red histogram) versus stars without debris discs (left) and stars with debris discs (right). Median values of the distributions are shown with vertical lines.

the SWDPs are mature stars (older than 1 Gyr), although low-mass planet host stars tend to group at old ages, > 5 Gyr, and the cool giant-planet stars span a larger range of 1 - 10 Gyr (Figure 10). This age behaviour reflects a bias introduced by current planet-detection techniques. Young stars are usually excluded from planet-search programmes owing to their high-levels of chromospheric activity, although much effort is being applied to overcome this problem (e.g. Dumusque et al. 2011a,b). Finally, we can exclude a dust luminosity evolution with age in the SWDP sample, in line with the results of Trilling et al. (2008) for solar-type stars surrounded by debris discs.

5. Conclusions

The number of debris disc stars known to host planets has increased in the past few years by a factor of $\sim 50\%$, particularly those associated with low-mass planets. This has motivated us to revisit the properties of these stars and to compare them with

stars with planets, stars with debris discs, and stars with neither debris nor planets.

We have identified a transition toward higher metallicities from SWODs to SWPs. The SWDs have a metallicity distribution similar to those of SWODs, although the distribution of the first ones might be slightly shifted towards higher metallicities. The SWDPs follow the same metallicity trend as SWPs, irrespective of whether the planets are low-mass or gas giants; thus, it is the planet which reveals the metallicity of the corresponding stars. There is a high rate of incidence of multiplanet systems in SWDPs. Their innermost planets are usually cool giants, but the planets are close-in when the debris disc stars only host low-mass planets. It cannot be excluded that this latter result could be biased by the planet detection techniques. These results support the scenario of core accretion for planet formation and the previous view that the mass of solids in proto-planetary discs is the main factor determining the outcome of planet formation processes.

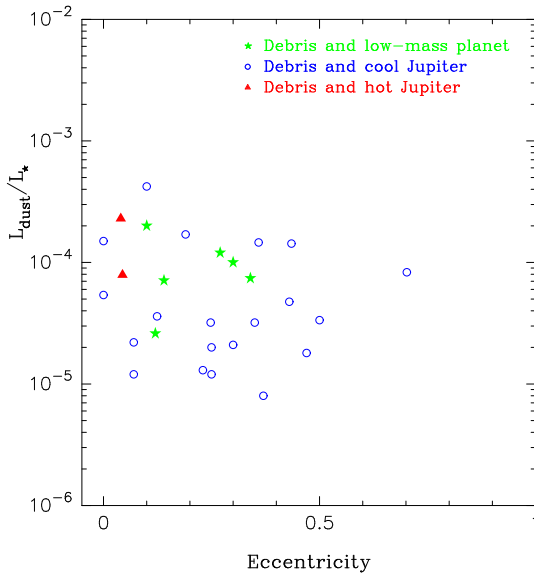


Fig. 9. Fractional dust luminosity, $L_{\text{dust}}/L_{\star}$, versus eccentricity.

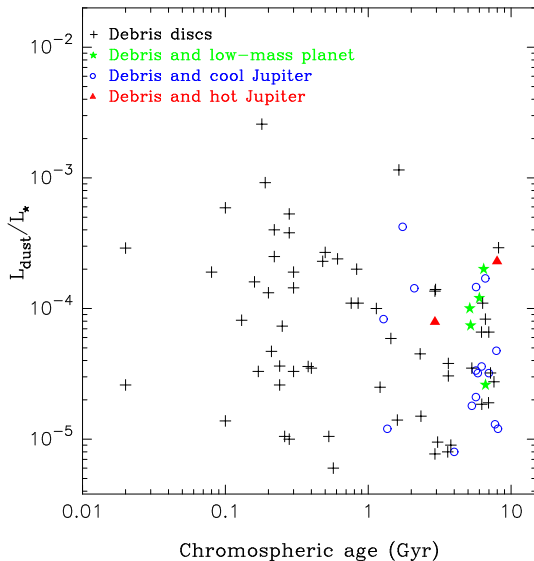


Fig. 10. Fractional dust luminosity, $L_{\text{dust}}/L_{\star}$, versus stellar age.

In addition, we have found that debris disc stars hosting cool giant planets tend to have the lowest dust luminosities, and that there is an anticorrelation between the dust luminosity and the innermost planet eccentricity. A plausible explanation of these suggested trends is provided by recent simulations of dynamical instabilities produced by eccentric giant planets. These apparent trends will likely be either confirmed or rejected by the various programmes dealing with planets and debris discs, currently being carried out with the *Herschel Space Observatory*, together with the expected detection of further planets, particularly low-mass planets, around the debris disc stars.

Finally, no other trend has been found relating debris disc and planet (e.g. period or semimajor axis) properties.

Acknowledgements. This work was supported by the Spanish Ministerio de Ciencia e Innovación (MICINN), Plan Nacional de Astronomía y Astrofísica, under grant AYA2008-01727. J.M. acknowledges support from the Universidad Autónoma de Madrid (Department of Theoretical Physics). We sincerely appreciate the careful reading of the manuscript and the constructive comments of an anonymous referee.

References

- Allende Prieto, C., Barklem, P. S., Lambert, D. L., & Cunha, K. 2004, A&A, 420, 183
- Aumann, H. H., Beichman, C. A., Gillett, F. C., et al. 1984, ApJ, 278, L23
- Backman, D. E. & Paresce, F. 1993, in Protostars and Planets III, ed. E. H. Levy & J. I. Lunine, 1253–1304
- Beichman, C. A., Bryden, G., Rieke, G. H., et al. 2005, ApJ, 622, 1160
- Beichman, C. A., Bryden, G., Stapelfeldt, K. R., et al. 2006, ApJ, 652, 1674
- Benítez, N., Maíz-Apellániz, J., & Canelles, M. 2002, Physical Review Letters, 88, 081101
- Bryden, G., Beichman, C. A., Carpenter, J. M., et al. 2009, ApJ, 705, 1226
- Bryden, G., Beichman, C. A., Trilling, D. E., et al. 2006, ApJ, 636, 1098
- Chavero, C., Gómez, M., Whitney, B. A., & Saffe, C. 2006, A&A, 452, 921
- Chen, C. H., Patten, B. M., Werner, M. W., et al. 2005, ApJ, 634, 1372
- Currie, T. 2009, ApJ, 694, L171
- Dodson-Robinson, S. E., Beichman, C. A., Carpenter, J. M., & Bryden, G. 2011, AJ, 141, 11
- Dumusque, X., Santos, N. C., Udry, S., Lovis, C., & Bonfils, X. 2011a, A&A, 527, A82
- Dumusque, X., Udry, S., Lovis, C., Santos, N. C., & Monteiro, M. J. P. F. G. 2011b, A&A, 525, A140
- Fischer, D. A. & Valenti, J. 2005, ApJ, 622, 1102
- Frandsen, S. & Lindberg, B. 1999, in Astrophysics with the NOT, ed. H. Karttunen & V. Pirola, 71
- Garnett, D. R. & Kobulnicky, H. A. 2000, ApJ, 532, 1192
- Ghezzi, L., Cunha, K., Schuler, S. C., & Smith, V. V. 2010a, ApJ, 725, 721
- Ghezzi, L., Cunha, K., Smith, V. V., et al. 2010b, ApJ, 720, 1290
- Gratton, R. G., Bonanno, G., Bruno, P., et al. 2001, Experimental Astronomy, 12, 107
- Greaves, J. S., Fischer, D. A., & Wyatt, M. C. 2006, MNRAS, 366, 283
- Greaves, J. S., Fischer, D. A., Wyatt, M. C., Beichman, C. A., & Bryden, G. 2007, MNRAS, 378, L1
- Habing, H. J., Dominik, C., Jourdain de Muizon, M., et al. 2001, A&A, 365, 545
- Hekker, S. & Meléndez, J. 2007, A&A, 475, 1003
- Hubickyj, O., Bodenheimer, P., & Lissauer, J. J. 2005, Icarus, 179, 415
- Ida, S. & Lin, D. N. C. 2004, ApJ, 616, 567
- Koerner, D. W., Kim, S., Trilling, D. E., et al. 2010, ApJ, 710, L26
- Kóspál, Á., Ardila, D. R., Moór, A., & Ábrahám, P. 2009, ApJ, 700, L73
- Maíz-Apellániz, J. 2001, ApJ, 560, L83
- Maldonado, J., Martínez-Arnáiz, R. M., Eiroa, C., Montes, D., & Montesinos, B. 2010, A&A, 521, A12
- Mamajek, E. E. & Hillenbrand, L. A. 2008, ApJ, 687, 1264
- Martínez-Arnáiz, R., Maldonado, J., Montes, D., Eiroa, C., & Montesinos, B. 2010, A&A, 520, A79
- Matteucci, F. & Greggio, L. 1986, A&A, 154, 279
- Matteucci, F. & Recchi, S. 2001, ApJ, 558, 351
- Matteucci, F., Spitoni, E., Recchi, S., & Valiante, R. 2009, A&A, 501, 531
- Mayor, M., Marmier, M., Lovis, C., et al. 2011, ArXiv e-prints
- Montes, D., López-Santiago, J., Gálvez, M. C., et al. 2001, MNRAS, 328, 45
- Moór, A., Ábrahám, P., Derekas, A., et al. 2006, ApJ, 644, 525
- Moór, A., Pascucci, I., Kóspál, Á., et al. 2011, ApJS, 193, 4
- Mordasini, C., Alibert, Y., & Benz, W. 2009, A&A, 501, 1139
- Mordasini, C., Alibert, Y., Benz, W., Klahr, H., & Henning, T. 2012, ArXiv e-prints
- Moro-Martín, A., Carpenter, J. M., Meyer, M. R., et al. 2007, ApJ, 658, 1312
- Nordström, B., Mayor, M., Andersen, J., et al. 2004, A&A, 418, 989
- Pasquini, L., Döllinger, M. P., Weiss, A., et al. 2007, A&A, 473, 979
- Peacock, J. A. 1983, MNRAS, 202, 615
- Pfeiffer, M. J., Frank, C., Baumueller, D., Fuhrmann, K., & Gehren, T. 1998, A&AS, 130, 381
- Plavchan, P., Werner, M. W., Chen, C. H., et al. 2009, The Astrophysical Journal, 698, 1068
- Pollack, J. B., Hubickyj, O., Bodenheimer, P., et al. 1996, Icarus, 124, 62
- Raymond, S. N., Armitage, P. J., Moro-Martín, A., et al. 2011, A&A, 530, A62
- Rhee, J. H., Song, I., Zuckerman, B., & McElwain, M. 2007, ApJ, 660, 1556
- Santos, N. C., Israeli, G., & Mayor, M. 2004, A&A, 415, 1153
- Smith, P. S., Hines, D. C., Low, F. J., et al. 2006, ApJ, 644, L125
- Sousa, S. G., Santos, N. C., Israeli, G., Mayor, M., & Udry, S. 2011, A&A, 533, A141
- Sousa, S. G., Santos, N. C., Mayor, M., et al. 2008, A&A, 487, 373
- Spangler, C., Sargent, A. I., Silverstone, M. D., Becklin, E. E., & Zuckerman, B. 2001, ApJ, 555, 932
- Takeda, Y., Ohkubo, M., & Sadakane, K. 2002, PASJ, 54, 451
- Takeda, Y., Sato, B., Kambe, E., et al. 2005, PASJ, 57, 109
- Tanner, A., Beichman, C., Bryden, G., Lisse, C., & Lawler, S. 2009, ApJ, 704, 109
- Timmes, F. X., Woosley, S. E., & Weaver, T. A. 1995, ApJS, 98, 617

Table A.1. Results of the K-S tests performed in this work.

Sample 1	Sample 2	n_1	n_2	n_{eff}	H_0^{\ddagger}	p	D
SWDs*	SWODs*	35	58	22	0	0.94	0.11
SWDs [#]	SWODs [#]	107	145	62	0	0.09	0.16
SWDPs	SWODs	29	145	24	1	$\sim 10^{-3}$	0.40
SWDPs	SWDs	29	107	23	1	7×10^{-3}	0.34
SWDPs	SWPs	29	120	24	0	0.49	0.17
SWPs	SWODs	120	145	66	1	$\sim 10^{-11}$	0.43
SWPs	SWDs	120	107	57	1	$\sim 10^{-10}$	0.44

\ddagger : 0: Accept null hypothesis; 1: Reject null hypothesis

*: Homogeneous samples; #: Full samples

\dagger : Only stars with giant planets considered

- Trilling, D. E., Bryden, G., Beichman, C. A., et al. 2008, ApJ, 674, 1086
 Trilling, D. E., Stansberry, J. A., Stapelfeldt, K. R., et al. 2007, ApJ, 658, 1289
 Valenti, J. A. & Fischer, D. A. 2005, ApJS, 159, 141
 van Leeuwen, F. v. 2007, Hipparcos, the New Reduction of the Raw Data (XXXII, 449 p., Hardcover, ISBN: 978-1-4020-6341-1: Astrophysics and Space Science Library , Vol. 350)
 Wright, J. T., Upadhyay, S., Marcy, G. W., et al. 2009, ApJ, 693, 1084

Appendix A: Results of the Kolmogorov-Smirnov tests

The Kolmogorov-Smirnov test (hereafter K-S test) is widely used to study the significance of the difference between two data samples (e.g. Peacock 1983). It is based on the maximum deviation between the empirical distribution functions of both samples

$$D = \max|F_1(x) - F_2(x)|, \quad (\text{A.1})$$

where $F_1(x)$ and $F_2(x)$ are the empirical distribution functions of the first and second samples respectively, and are given by

$$F(x) = \frac{n(x_i \leq x)}{N}. \quad (\text{A.2})$$

The K-S test tests the null hypothesis H_0 that $F_1(x)=F_2(x)$, i.e., both samples come from the same underlying continuous distribution, which is accepted if

$$\max|F_1(x) - F_2(x)| < C_{\frac{\alpha}{2}, n_1, n_2} \quad (\text{A.3})$$

where n_1 and n_2 are the sizes of the samples, α is the confidence level, and C the corresponding critical values of the K-S distribution.

Through this paper, we perform several K-S tests between the different samples studied. Results are given in Table A.1, where the “asymptotic p value” is also given. It provides an estimate of the likelihood of the null hypothesis and is reasonable accurate for samples sizes for which

$$n_{\text{eff}} = \frac{n_1 \times n_2}{n_1 + n_2} \geq 4. \quad (\text{A.4})$$

All the tests were made at a confidence level $\alpha=0.02$.

1. Tables

Results produced in the framework of this work are only available in the electronic version of the corresponding paper or at the CDS via anonymous ftp to cdsarc.u-strasbg.fr (130.79.128.5) or via <http://cdsweb.u-strasbg.fr/cgi-bin/qcat?J/A+A/>

Table 1 lists the stars in the SWDs (stars with known debris discs) and SWODs (stars without debris discs) samples, as well as their properties: HIP number (column 1); HD number (column 2); Hipparcos spectral-type (column 3); distance in parsec (column 4); logAge(yr) (column 5); [Fe/H] and its reference (column 6); and references for debris disc detection (column 7). References for [Fe/H] are: (a) this work; (b) Valenti & Fischer (2005); (c) Nordström et al. (2004); metallicities taken from (b) and (c) are set on the metallicity scale of this work as described in Section 3.2. References in column 6 are as follows: (1) Habing et al. (2001); (2) Spangler et al. (2001); (3) Chen et al. (2005); (4) Beichman et al. (2006); (5) Bryden et al. (2006); (6) Moór et al. (2006); (7) Smith et al. (2006); (8) Rhee et al. (2007); (9) Trilling et al. (2008); (10) Kóspál et al. (2009); (11) Plavchan et al. (2009); (12) Tanner et al. (2009); (13) Koerner et al. (2010); (14) Moór et al. (2011).

Table 5 contains: HIP number (column 1); HD number (column 2); Hipparcos spectral-type (column 3); effective temperature in kelvin (column 4); logarithm of the surface gravity in cm s^{-2} (column 5); microturbulent velocity in km s^{-1} (column 6); final metallicity in dex (column 7); mean iron abundance derived from Fe I lines (column 8) in the usual scale ($A(\text{Fe}) = \log[(N_{\text{Fe}}/N_{\text{H}}) + 12]$); number of Fe I lines used (column 9); mean iron abundance derived from Fe II lines (column 10); number of Fe II lines used (column 11); and spectrograph (column 12). Each measured quantity is accompanied by its corresponding uncertainty.

Table 1 The SWDs and SWODs samples.

HIP	HD	SpType	V	distance (pc)	log(Age) (yr)	[Fe/H] [†] (dex)	Ref
Stars with known debris discs.							
171	224930	G3V	5.80	12.17	9.60	-0.72 (a)	13
490	105	G0V	7.51	39.39	8.34	-0.03 (b)	2
544	166	K0V	6.07	13.67	9.16	0.15 (a)	5
682	377	G2V	7.59	39.08	8.34	0.12 (b)	6
1481	1466	F8/G0	7.46	41.55	8.34	-0.22 (c)	7
1598	1562	G0	6.97	24.80	9.79	-0.32 (a)	13
1599	1581	F9V	4.23	8.59	9.58	-0.29 (a)	9
2843	3296	F5	6.72	45.05		0.02 (c)	9
3810	4676	F8V	5.07	23.45	9.71	0.00 (c)	13
4148	5133	K2V	7.15	14.17	9.56	-0.16 (b)	13
5336	6582	G5V	5.17	7.55	9.69	-0.89 (a)	13
5862	7570	F8V	4.97	15.10	9.62	0.17 (a)	10
5944	7590	G0	6.59	23.20	8.70	-0.02 (a)	11
6878	8907	F8	6.66	34.77	8.78	-0.09 (b)	6
7576	10008	G5	7.66	23.96	8.10	0.08 (a)	11
8102	10700	G8V	3.49	3.65	9.77	-0.43 (a)	1
11160	15060	F5	7.02	75.99		-0.08 (c)	14
12623	16739	F9V	4.91	24.19	9.83	0.21 (c)	13
13402	17925	K1V	6.05	10.35	8.24	0.08 (a)	1
13642	18143	K2	7.52	23.52		0.35 (a)	13
15371	20807	G1V	5.24	12.03	9.49	-0.16 (a)	9
16852	22484	F9V	4.29	13.97	9.88	-0.07 (a)	9
17439	23484	K1V	6.99	16.03	8.88	0.04 (b)	13
18859	25457	F5V	5.38	18.84	9.06	-0.04 (c)	6
19335	25998	F7V	5.52	21.00	9.36	0.08 (c)	4
22263	30495	G3V	5.49	13.27	9.08	0.04 (a)	1
22295	32195	F7V	8.14	61.01		-0.07 (c)	14
23693	33262	F7V	4.71	11.64	8.76	-0.15 (c)	5
23816	33081	F7V	7.04	50.61		-0.13 (c)	14
24205	33636	G0	7.00	28.37	9.56	-0.15 (b)	9
24947	35114	F6V	7.39	48.31		-0.12 (c)	14
25486	35850	F7V	6.30	27.04	7.29	-0.09 (b)	2
26779	37394	K1V	6.21	12.28	8.93	0.14 (a)	12
27072	38393	F7V	3.59	8.93	9.47	-0.09 (a)	8
27980	39833	G0III	7.65	41.22		0.20 (c)	8
29568	43162	G5V	6.37	16.72	8.45	0.00 (a)	10
31711	48189	G1/G2V	6.15	21.29	8.02	-0.18 (c)	11
32480	48682	G0V	5.24	16.72	9.80	0.16 (a)	4
32775	50571	F7III-IV	6.11	33.62	8.93	0.08 (c)	6
33690	53143	K0IV-V	6.81	18.33	8.92	0.28 (a)	6
34819	55052	F5IV	5.85	109.77		0.07 (c)	8
36515	59967	G3V	6.66	21.82	8.39	-0.19 (c)	11
36827	60491	K2V	8.16	24.56	7.92	-0.18 (a)	13
36906	60234	G0	7.68	133.87		0.15 (c)	8
36948	61005	G3/G5V	8.23	35.35	8.27	-0.13 (c)	8
42333	73350	G0	6.74	23.98	8.48	0.07 (a)	11
42430	73752	G3/G5V	5.05	19.38	9.86	0.39 (c)	8
42438	72905	G1.5V	5.63	14.35	8.41	-0.02 (a)	2
43625	75616	F5	6.92	35.42		-0.26 (c)	9
43726	76151	G3V	6.01	17.39	9.20	0.23 (a)	12
50384	89125	F8V	5.81	22.82	9.84	-0.27 (a)	13
52462	92945	K1V	7.72	21.40	8.45	-0.15 (b)	3
56830	101259	G6/G8V	6.40	63.09		-0.72 (b)	9
59422	105912	F5	6.95	49.68		-0.01 (c)	9
60025	107067	F8	8.69	65.96	9.22	-0.03 (c)	2
60074	107146	G2V	7.04	27.46	8.28	-0.07 (b)	6
60582	108102	F8	8.12	95.15	8.00	-0.07 (c)	2
62207	110897	G0V	5.95	17.38	9.80	-0.53 (a)	9
63584	113337	F6V	6.01	36.89		0.13 (c)	8
66704	119124	F8V	6.31	25.33	8.38	-0.16 (c)	3
66765	118972	K1V	6.92	15.65	8.60	-0.11 (b)	9
66781	119332	K0IV-V	7.77	24.63		-0.07 (a)	13
68101	121384	G8V	6.00	38.70		-0.53 (b)	8
68380	122106	F8V	6.36	77.52		0.20 (c)	6
68593	122652	F8	7.16	39.29	9.47	-0.02 (b)	8

Table 1 Continued

HIP	HD	SpType	V	distance (pc)	log(Age) (yr)	[Fe/H] [†] (dex)	Ref
69682	124718	G5V	8.89	63.17		-0.03 (c)	8
69989	125451	F5IV	5.41	26.10		0.07 (c)	2
70344	126265	G2III	7.21	70.42		0.12 (c)	8
72848	131511	K2V	6.00	11.51	8.84	0.13 (a)	13
73869	134319	G5	8.40	44.74	8.20	-0.15 (b)	2
74702	135599	K0	6.92	15.85	8.31	-0.13 (a)	11
74975	136202	F8III-IV	5.04	25.38	9.92	0.02 (c)	13
76375	139323	K3V	7.65	22.38		0.30 (b)	8
76635	139590	G0V	7.50	55.77		0.08 (c)	8
76829	139664	F5IV-V	4.64	17.44		-0.05 (c)	1
79492	145958	G8V	6.68	23.79	9.73	-0.09 (b)	13
81800	151044	F8V	6.48	29.33	9.82	-0.03 (b)	1
85235	158633	K0V	6.44	12.80	9.73	-0.44 (a)	4
88399	164249	F5V	7.01	48.15		-0.07 (c)	6
88745	165908	F7V	5.05	15.64	9.37	-0.60 (a)	13
89770	169666	F5	6.68	53.22		0.02 (c)	6
90936	170773	F5V	6.22	36.98	8.44	0.00 (c)	6
93815	177171	F7	5.17	56.72		0.01 (c)	7
94050	177996	K1V	7.89	33.84	8.33	-0.23 (c)	2
94858	180134	F7	6.36	45.07		-0.12 (c)	7
95270	181327	F5/F6V	7.04	51.81		0.14 (c)	6
96258	184960	F7V	5.71	25.11		-0.17 (c)	2
99273	191089	F5V	7.18	52.22		-0.09 (c)	6
99316	191499	K0	7.56	23.64		-0.16 (a)	13
102626	197890	K0V	9.44	52.19		-1.49 (c)	11
103389	199260	F7V	5.70	21.97	8.48	-0.11 (c)	4
104239	200968	K1V	7.12	17.58	9.47	-0.01 (a)	13
105184	202628	G5V	6.75	24.42	9.47	-0.02 (b)	13
105388	202917	G5V	8.65	42.97	7.18	0.03 (b)	2
107022	205536	G8V	7.07	22.02	9.91	-0.04 (b)	8
107350	206860	G0V	5.96	17.88	8.73	-0.20 (a)	9
107412	206893	F5V	6.69	38.34	8.68	-0.01 (c)	6
107649	207129	G2V	5.57	15.99	9.84	-0.06 (b)	1
108028	208038	K0	8.18	23.04	8.48	-0.02 (a)	13
108809	209253	F6/F7V	6.63	30.14	8.39	-0.03 (b)	2
110753	212695	F5	6.94	46.49		-0.02 (c)	9
111170	213429	F7V	6.15	25.41	9.56	0.02 (c)	14
114236	218340	G3	8.44	56.59		0.09 (a)	7
114924	219623	F7V	5.58	20.50		-0.03 (c)	4
114948	219482	F7V	5.64	20.54	8.59	-0.15 (c)	4
117712	223778	K3V	6.36	10.89	8.93	-0.68 (c)	13
3670		F5V	8.23			-0.07 (c)	14

Stars without debris discs.

394	225239	G2V	6.09	39.18		-0.41 (c)	
462	63	F5	7.13	50.66		-0.09 (c)	
910	693	F5V	4.89	18.75	9.48	-0.32 (c)	
1573	1539	F5	7.03	43.69		-0.04 (c)	
2802	3302	F6V	5.51	34.82	8.50	0.04 (c)	
3170	3823	G1V	5.89	24.96	9.63	-0.26 (b)	
3185	3795	G3/G5V	6.14	28.89	9.82	-0.49 (b)	
3236	3861	F5	6.52	33.44	9.25	0.05 (b)	
3559	4307	G2V	6.15	31.00	9.89	-0.22 (b)	
3765	4628	K2V	5.74	7.45		-0.24 (a)	
3909	4813	F7IV-V	5.17	15.75	2.93	-0.16 (a)	
7601	10800	G2V	5.88	27.38	9.09	-0.11 (c)	
7981	10476	K1V	5.24	7.53		-0.03 (a)	
8486	11131	G0	6.72	22.56	7.72	-0.03 (a)	
10306	13555	F5V	5.23	28.87		-0.21 (c)	
10798	14412	G8V	6.33	12.67	9.61	-0.46 (a)	
11072	14802	G2V	5.19	21.96	9.80	-0.06 (a)	
11548	15335	G0V	5.89	31.41		-0.24 (b)	
11783	15798	F5V	4.74	26.70	9.26	-0.26 (c)	
12114	16160	K3V	5.79	7.18		-0.19 (a)	
12777	16895	F7V	4.10	11.13	9.90	0.12 (a)	
14632	19373	G0V	4.05	10.54	9.82	0.11 (a)	
15330	20766	G2V	5.53	12.01	9.61	-0.21 (a)	
15457	20630	G5Vvar	4.84	9.14	8.54	0.09 (a)	

Table 1 Continued

HIP	HD	SpType	V	distance (pc)	log(Age) (yr)	[Fe/H] [†] (dex)	Ref
17378	23249	K0IV	3.52	9.04		0.03 (b)	
19855	26913	G5IV	6.94	21.06	8.45	-0.11 (c)	
22449	30652	F6V	3.19	8.07	9.48	-0.01 (b)	
23311	32147	K3V	6.22	8.71		0.29 (a)	
24786	34721	G0V	5.96	25.03	9.79	-0.24 (a)	
24813	34411	G0V	4.69	12.63	9.83	0.08 (a)	
25278	35296	F8V	5.00	14.39	8.41	-0.09 (c)	
27913	39587	G0V	4.39	8.66	8.75	-0.09 (a)	
28954	41593	K0	6.76	15.27	8.70	0.19 (a)	
29271	43834	G5V	5.08	10.20	9.74	0.12 (a)	
32984	50281	K3V	6.58	8.71		-0.02 (b)	
33277	50692	G0V	5.74	17.24	9.74	-0.11 (a)	
34017	52711	G4V	5.93	19.13	9.74	-0.14 (a)	
35136	55575	G0V	5.54	16.89	9.72	-0.36 (a)	
36439	58855	F6V	5.35	20.24		-0.23 (c)	
37283	60912	F5	6.89	45.50		-0.07 (c)	
37853	63077	G0V	5.36	15.21	9.55	-0.72 (c)	
38172	63333	F5	7.09	43.08		-0.38 (c)	
39780	67228	G2IV	5.30	23.29	9.69	0.19 (b)	
39903	68456	F5V	4.74	19.98	8.09	-0.17 (c)	
40843	69897	F6V	5.13	18.27		-0.39 (a)	
41226	70843	F5	7.06	46.30		0.14 (b)	
41484	71148	G5V	6.32	22.25		0.01 (a)	
41573	71640	F5	7.40	44.74		-0.18 (c)	
41926	72673	K0V	6.38	12.21	9.75	-0.40 (b)	
42074	72760	G5	7.32	21.14	8.03	0.01 (a)	
42808	74576	K2V	6.58	11.14	8.73	-0.16 (a)	
44728	77967	F0	6.61	43.25		-0.36 (c)	
44897	78366	F9V	5.95	19.19	8.70	0.03 (b)	
45699	80218	F5	6.61	40.65		-0.21 (c)	
47403	83451	F5	7.12	49.04		-0.06 (c)	
47436	83525	F5	6.90	48.97		-0.07 (c)	
47592	84117	G0V	4.93	15.01	9.62	-0.21 (a)	
48113	84737	G2V	5.08	18.37	9.87	0.10 (a)	
48768	86147	F5	6.70	47.01		-0.01 (c)	
50366	88984	F5	7.30	51.15		-0.21 (c)	
51459	90839	F8V	4.82	12.78	9.47	-0.15 (a)	
52574	93081	F5	7.09	48.38		-0.22 (c)	
53252	94388	F6V	5.23	30.81	9.54	0.24 (c)	
54745	97334	G0V	6.41	21.93	8.03	-0.01 (a)	
55666	99126	F5	6.94	49.75		-0.09 (c)	
56186	100067	F5	7.17	39.95		-0.32 (c)	
56452	100623	K0V	5.96	9.56	9.61	-0.38 (a)	
56997	101501	G8Vvar	5.31	9.61	8.91	0.01 (a)	
57507	102438	G5V	6.48	17.47	9.72	-0.28 (b)	
57757	102870	F8V	3.59	10.93	9.81	0.09 (a)	
57939	103095	G8Vp	6.42	9.09	9.67	-1.12 (a)	
58268	103773	F5	6.73	46.45		0.05 (c)	
58803	104731	F6V	5.15	25.32	8.56	-0.01 (c)	
61100	109011	K2V	8.08	25.10		-0.34 (a)	
61578	109756	F5	6.95	48.52		-0.15 (c)	
62523	111395	G7V	6.29	16.93	8.57	0.22 (a)	
62636	111545	F5	6.99	47.76		-0.02 (c)	
63033	112164	G2IV	5.89	40.10		0.20 (c)	
63742	113449	G5V	7.69	21.70	8.28	-0.17 (a)	
64394	114710	G0V	4.23	9.13	9.89	0.11 (a)	
64408	114613	G3V	4.85	20.67		0.18 (b)	
64792	115383	G0Vs	5.19	17.56	8.61	0.24 (a)	
65515	116956	G9IV-V	7.29	21.59	7.84	0.03 (a)	
65530	117043	G6V	6.50	21.17		0.29 (a)	
67195	120005	F5	6.51	43.73		0.05 (c)	
67620	120690	G5V	6.43	19.47	9.31	0.05 (a)	
69040	123691	F2	6.80	53.02		-0.08 (c)	
69090	122862	G1V	6.02	28.50	9.82	-0.15 (b)	
70497	126660	F7V	4.04	14.53	9.03	-0.08 (c)	
70873	127334	G5V	6.36	23.74		0.25 (b)	
71743	128987	G6V	7.24	23.67	8.81	0.01 (a)	

Table 1 Continued

HIP	HD	SpType	V	distance (pc)	log(Age) (yr)	[Fe/H] [†] (dex)	Ref
72130	130460	F5	7.22	49.12		-0.01 (c)	
72567	130948	G2V	5.86	18.17	8.28	-0.01 (b)	
72573	133002	F9V	5.63	43.29		-0.41 (c)	
73996	134083	F5V	4.93	19.55	9.60	0.05 (b)	
74605	136064	F9IV	5.15	25.34	9.46	-0.03 (c)	
77372	141128	F5	7.00	49.24		-0.19 (c)	
77408	141272	G8V	7.44	21.29	8.29	-0.14 (a)	
77760	142373	F9V	4.60	15.89	9.87	-0.50 (a)	
77801	142267	G0IV	6.07	17.35	9.60	-0.50 (a)	
77838	143105	F5	6.76	48.66		0.03 (c)	
78072	142860	F6V	3.85	11.25		-0.17 (b)	
79672	146233	G1V	5.49	13.90	9.63	0.04 (a)	
81300	149661	K2V	5.77	9.75	9.36	0.05 (a)	
82588	152391	G8V	6.65	17.25	8.44	0.04 (a)	
84862	157214	G0V	5.38	14.33	9.77	-0.41 (a)	
88972	166620	K2V	6.38	11.02	9.76	-0.07 (b)	
89348	168151	F5V	4.99	22.92	9.62	-0.17 (c)	
90485	169830	F8V	5.90	36.60	9.81	0.09 (b)	
91120	171886	F5	7.16	49.43		-0.30 (c)	
91438	172051	G5V	5.85	13.08	9.66	-0.21 (a)	
92043	173667	F6V	4.19	19.21	9.68	0.12 (b)	
93252	176441	F5	7.06	46.77		-0.16 (c)	
93858	177565	G8V	6.15	16.95	9.78	0.07 (b)	
94346	180161	G8V	7.04	20.02	8.84	0.18 (a)	
94981	181655	G8V	6.29	25.39	9.79	0.02 (b)	
95149	181321	G1/G2V	6.48	18.83	8.39	-0.21 (c)	
96100	185144	K0V	4.67	5.75	9.56	-0.26 (a)	
96895	186408	G2V	5.99	21.08	9.84	0.02 (a)	
97675	187691	F8V	5.12	19.19	9.85	0.13 (b)	
98066	188376	G3/G5III	4.70	25.99	9.87	0.06 (c)	
98819	190406	G1V	5.80	17.77	9.50	0.12 (a)	
98959	189567	G2V	6.07	17.73	9.61	-0.22 (b)	
99240	190248	G5IV-Vvar	3.55	6.11	9.82	0.36 (a)	
99461	191408	K2V	5.32	6.02		-0.40 (b)	
100017	193664	G3V	5.91	17.57	9.58	-0.14 (b)	
101983	196378	F8V	5.11	24.66	9.57	-0.39 (b)	
101997	196761	G8/K0V	6.36	14.38	9.72	-0.30 (b)	
102485	197692	F5V	4.13	14.68	8.49	0.03 (c)	
103931	200433	F5	6.91	47.37		-0.05 (c)	
105202	202884	F5	7.27	41.81		-0.27 (c)	
105858	203608	F6V	4.21	9.26	8.76	-0.84 (a)	
109422	210302	F6V	4.94	18.28	9.55	0.09 (b)	
109821	210918	G5V	6.23	22.05		-0.09 (b)	
110649	212330	F9V	5.31	20.56		0.00 (b)	
112447	215648	F7V	4.20	16.30		-0.20 (b)	
113829	217813	G5V	6.65	24.72		0.02 (b)	
114622	219134	K3Vvar	5.57	6.55		0.10 (b)	
115220	219983	F2	6.64	48.73		-0.12 (c)	
115331	220182	K1V	7.36	21.52	7.56	0.11 (a)	
116250	221420	G2V	5.82	31.44		0.33 (b)	
116613	222143	G5	6.58	23.33	9.08	0.14 (a)	
116745	222237	K3V	7.09	11.42		-0.24 (b)	
116771	222368	F7V	4.13	13.71		-0.13 (a)	
116906	222582	G5	7.68	41.77		-0.03 (b)	

Table 5 Continued

HIP	HD	SpType	T _{eff} (K)	log g (cm s ⁻²)	ξ_t (km s ⁻¹)	[Fe/H] dex	$\langle A(\text{Fe I}) \rangle$	n _I	$\langle A(\text{Fe II}) \rangle$	n _{II}	Spec. [†]
(1)	(2)	(3)	(4)	(5)	(6)	(7)	(8)	(9)	(10)	(11)	(12)
10798	14412	G8V	5359 ± 25	4.59 ± 0.07	0.48 ± 0.39	-0.46 ± 0.05	7.04 ± 0.06	62	7.04 ± 0.06	11	4
11072	14802	G2V	5853 ± 49	3.99 ± 0.15	1.28 ± 0.15	-0.06 ± 0.05	7.44 ± 0.06	43	7.44 ± 0.08	9	6
12114	16160	K3V	4857 ± 52	4.54 ± 0.12	0.04 ± 0.43	-0.19 ± 0.10	7.32 ± 0.09	59	7.30 ± 0.16	9	1
12777	16895	F7V	6304 ± 76	4.54 ± 0.20	1.38 ± 0.35	0.12 ± 0.05	7.62 ± 0.06	43	7.62 ± 0.07	12	4
14632	19373	G0V	5975 ± 67	4.14 ± 0.21	1.32 ± 0.16	0.11 ± 0.05	7.61 ± 0.06	60	7.61 ± 0.08	13	4
15330	20766	G2V	5719 ± 29	4.63 ± 0.08	0.87 ± 0.18	-0.21 ± 0.04	7.29 ± 0.05	54	7.29 ± 0.06	13	5
15457	20630	G5Vvar	5718 ± 50	4.52 ± 0.12	0.94 ± 0.26	0.09 ± 0.04	7.59 ± 0.06	61	7.59 ± 0.06	13	4
23311	32147	K3V	4746 ± 30	4.55 ± 0.09	0.50 ± 0.25	0.29 ± 0.02	7.80 ± 0.02	60	7.79 ± 0.05	10	4
24786	34721	G0V	5716 ± 70	3.54 ± 0.25	1.22 ± 0.27	-0.24 ± 0.09	7.26 ± 0.12	39	7.26 ± 0.14	5	2
24813	34411	G0V	5871 ± 36	4.40 ± 0.11	1.24 ± 0.19	0.08 ± 0.04	7.58 ± 0.05	62	7.59 ± 0.05	13	4
27913	39587	G0V	5813 ± 26	4.45 ± 0.08	1.12 ± 0.18	-0.09 ± 0.04	7.41 ± 0.05	43	7.41 ± 0.05	12	4
28954	41593	K0	5515 ± 31	4.67 ± 0.09	1.01 ± 0.32	0.19 ± 0.04	7.69 ± 0.06	52	7.70 ± 0.05	12	1
29271	43834	G8V	5649 ± 37	4.60 ± 0.10	0.80 ± 0.31	0.12 ± 0.05	7.62 ± 0.06	62	7.62 ± 0.06	13	5
33277	50692	G0V	5870 ± 31	4.57 ± 0.09	0.83 ± 0.23	-0.11 ± 0.04	7.39 ± 0.05	54	7.39 ± 0.05	11	1
34017	52711	G4V	5797 ± 37	4.20 ± 0.11	0.98 ± 0.18	-0.14 ± 0.05	7.36 ± 0.06	62	7.36 ± 0.07	13	1
35136	55575	G0V	5821 ± 46	4.29 ± 0.13	1.32 ± 0.22	-0.36 ± 0.06	7.14 ± 0.07	59	7.14 ± 0.09	13	1
40843	69897	F6V	6041 ± 69	3.79 ± 0.18	1.51 ± 0.35	-0.39 ± 0.09	7.11 ± 0.10	42	7.11 ± 0.13	13	1
41484	71148	G5V	5838 ± 39	4.58 ± 0.12	1.30 ± 0.33	0.01 ± 0.05	7.51 ± 0.06	57	7.52 ± 0.07	12	1
42074	72760	G5	5203 ± 40	4.62 ± 0.09	0.66 ± 0.37	0.01 ± 0.06	7.52 ± 0.07	52	7.51 ± 0.08	10	1
42808	74576	K2V	4915 ± 45	4.48 ± 0.11	1.05 ± 0.28	-0.16 ± 0.09	7.35 ± 0.11	51	7.34 ± 0.14	9	5
47592	84117	G0V	5991 ± 62	4.21 ± 0.17	1.89 ± 0.36	-0.21 ± 0.08	7.29 ± 0.10	36	7.29 ± 0.11	6	2
48113	84737	G2V	5821 ± 25	4.06 ± 0.08	1.15 ± 0.12	0.10 ± 0.03	7.60 ± 0.03	57	7.60 ± 0.04	11	1
51459	90839	F8V	6050 ± 28	4.29 ± 0.08	1.28 ± 0.15	-0.15 ± 0.04	7.35 ± 0.04	62	7.35 ± 0.05	13	4
54745	97334	G0V	5865 ± 45	4.46 ± 0.13	1.48 ± 0.34	-0.01 ± 0.06	7.49 ± 0.07	44	7.49 ± 0.08	10	1
56452	100623	K0V	5139 ± 53	4.55 ± 0.12	0.70 ± 0.28	-0.38 ± 0.07	7.12 ± 0.08	58	7.12 ± 0.11	10	4
56997	101501	G8V	5591 ± 49	4.60 ± 0.14	0.93 ± 0.20	0.01 ± 0.04	7.50 ± 0.04	63	7.51 ± 0.06	13	4
57757	102870	F8V	6044 ± 40	4.02 ± 0.12	1.41 ± 0.18	0.09 ± 0.04	7.59 ± 0.05	60	7.59 ± 0.06	12	4
57939	103095	G8V	5144 ± 77	4.05 ± 0.20	0.77 ± 0.49	-1.12 ± 0.25	6.38 ± 0.30	33	6.38 ± 0.39	6	1
61100	109011	K2V	4925 ± 48	4.38 ± 0.12	1.07 ± 0.29	-0.34 ± 0.11	7.16 ± 0.12	36	7.16 ± 0.17	8	1
62523	111395	G7V	5677 ± 33	4.65 ± 0.08	0.64 ± 0.20	0.22 ± 0.03	7.72 ± 0.04	58	7.72 ± 0.03	12	1
63742	113449	G5V	5050 ± 55	4.51 ± 0.13	0.96 ± 0.28	-0.17 ± 0.10	7.33 ± 0.12	49	7.33 ± 0.15	8	1
64394	114710	G0V	6023 ± 40	4.24 ± 0.11	1.03 ± 0.20	0.11 ± 0.03	7.61 ± 0.03	62	7.61 ± 0.05	13	4
64792	115383	G0Vs	6133 ± 50	4.63 ± 0.13	1.30 ± 0.26	0.24 ± 0.04	7.74 ± 0.05	53	7.74 ± 0.05	13	1
65515	116956	G9IV-V	5214 ± 34	4.65 ± 0.08	0.93 ± 0.31	0.03 ± 0.05	7.53 ± 0.07	49	7.53 ± 0.07	8	1
65530	117043	G6V	5610 ± 38	4.38 ± 0.11	0.73 ± 0.17	0.29 ± 0.03	7.79 ± 0.04	58	7.79 ± 0.03	13	1
67620	120690	G5V	5720 ± 33	4.63 ± 0.09	0.60 ± 0.39	0.05 ± 0.04	7.55 ± 0.06	49	7.54 ± 0.05	11	3
71743	128987	G6V	5511 ± 123	4.86 ± 0.29	0.80 ± 0.48	0.01 ± 0.11	7.51 ± 0.12	48	7.51 ± 0.16	5	2
77408	141272	G8V	5191 ± 31	4.64 ± 0.07	0.87 ± 0.21	-0.14 ± 0.05	7.37 ± 0.07	49	7.36 ± 0.08	10	1
77760	142373	F9V	5802 ± 65	4.14 ± 0.19	2.00 ± 0.38	-0.50 ± 0.07	7.00 ± 0.09	50	7.00 ± 0.11	13	1
77801	142267	G0IV	5698 ± 53	4.39 ± 0.17	1.14 ± 0.40	-0.50 ± 0.10	7.00 ± 0.13	42	7.00 ± 0.14	9	3
79672	146233	G1V	5804 ± 81	4.43 ± 0.20	1.01 ± 0.24	0.04 ± 0.06	7.54 ± 0.09	59	7.54 ± 0.09	12	4
81300	149661	K2V	5192 ± 57	4.65 ± 0.16	0.33 ± 0.46	0.05 ± 0.06	7.55 ± 0.07	55	7.55 ± 0.10	11	4
82588	152391	G8V	5442 ± 51	4.62 ± 0.16	0.34 ± 0.43	0.04 ± 0.05	7.54 ± 0.05	41	7.54 ± 0.07	13	1
84862	157214	G0V	5663 ± 34	4.40 ± 0.12	1.32 ± 0.34	-0.41 ± 0.05	7.09 ± 0.07	48	7.09 ± 0.08	10	3
91438	172051	G5V	5638 ± 27	4.65 ± 0.08	0.94 ± 0.29	-0.21 ± 0.04	7.29 ± 0.06	60	7.29 ± 0.06	13	5
94346	180161	G8	5344 ± 59	4.55 ± 0.12	0.71 ± 0.35	0.18 ± 0.06	7.68 ± 0.09	53	7.68 ± 0.08	10	1
96100	185144	K0V	5329 ± 72	4.54 ± 0.20	0.98 ± 0.35	-0.26 ± 0.12	7.24 ± 0.13	60	7.24 ± 0.18	13	4
96895	186408	G2V	5760 ± 74	4.35 ± 0.24	1.05 ± 0.18	0.02 ± 0.06	7.52 ± 0.08	53	7.52 ± 0.10	10	3
98819	190406	G1V	6067 ± 32	4.64 ± 0.08	1.20 ± 0.22	0.12 ± 0.03	7.62 ± 0.05	41	7.62 ± 0.04	5	2
99240	190248	G5IV-V	5603 ± 35	4.37 ± 0.11	0.87 ± 0.20	0.36 ± 0.02	7.86 ± 0.03	56	7.86 ± 0.02	13	5
105858	203608	F6V	5910 ± 38	4.12 ± 0.06	2.60 ± 0.20	-0.84 ± 0.04	6.66 ± 0.02	42	6.66 ± 0.07	13	5
115331	220182	K1V	5455 ± 48	4.65 ± 0.15	0.72 ± 0.26	0.11 ± 0.04	7.61 ± 0.05	39	7.61 ± 0.07	12	1
116613	222143	G5	5795 ± 35	4.41 ± 0.11	1.00 ± 0.27	0.14 ± 0.04	7.64 ± 0.06	61	7.64 ± 0.06	13	1
116771	222368	F7V	6221 ± 92	4.37 ± 0.22	2.38 ± 0.39	-0.13 ± 0.04	7.37 ± 0.10	55	7.37 ± 0.12	13	4

[†]Spectrograph: (1) CAHA/FOCES; (2) TNG/SARG; (3) NOT/FIES; (4) S⁴N-McD (5) S⁴N-FEROS; (6) ESO/FEROS ST-ECF Science Archive